ANTI-PLANE INTERACTION BETWEEN A CRACK AND AN ELLIPTICALLY CYLINDRICAL LAYERED MEDIA

C.K. Chao * A. Wikarta

Department of Mechanical Engineering
National Taiwan University of Science and Technology
Taipei, Taiwan 10607, R.O.C.

ABSTRACT

Anti-plane interaction of an elliptically cylindrical layered media with an arbitrarily oriented crack embedded in an infinite matrix, intermediate layer, or inner inclusion under a remote uniform shear load is considered in this paper. Based on the technique of conformal mapping and the method of analytical continuation in conjunction with the alternating technique, the solution for a screw dislocation in the inclusions and the matrix is first derived in a series form. The integral equations with logarithmic singular kernels for a line crack can easily be obtained by using the screw dislocation solutions as the Green's function together with the principle superposition. The stress intensity factors, which can properly reflect the interaction between a crack and an elliptically cylindrical layered media, are then obtained numerically in terms of the values of the dislocation density functions of the integral equations. The effects of material property combinations and geometric parameters on the normalized mode-III stress intensity factors are discussed in detail and shown in graphic form.

Keywords: Elliptically cylindrical layered media, Arbitrarily oriented crack, Conformal mapping, Mode-III stress intensity factors.

1. INTRODUCTION

The problem of anti-plane interaction of a crack with a reinforced elliptical hole embedded in an infinite matrix has been recently solved by Chao *et al*. [1]. It was shown that the solution of the problem with crack embedded in matrix is done by integrating screw dislocation distribution along the prospective site of the crack and applied superposition technique. The solution for a screw dislocation is obtained from the method of conformal mapping and the technique of analytical continuation that is alternately applied across two different interfaces. The purpose of the present paper is to extend the above mentioned methodology to the case where an elliptically cylindrical layered media interacts with a crack located either in the matrix or in the inclusions.

One of the major difficulties for solving a multilayered elliptic medium is non-conformal inside the elliptic inclusion when we apply the mapping function from an elliptic boundary onto a unit circle. To overcome this difficulty, a restricted condition is applied to remedy the discontinuity problem which occurs when the transformation is required to be single-valued and conformal in the entire domain including the matrix and inclusion [2]. By applying this technique, Ru [3], Ru *et al.* [4], and Shen *et al*. [5] have modeled the three phase elliptical inclusion. These authors found that the solution is in good agreement with known results.

In this paper, the interaction between an elliptically cylindrical layered media and an arbitrarily oriented crack embedded in an infinite matrix, intermediate layer, and inner inclusion is considered. The solution for a screw dislocation in the inclusions and the matrix is first derived in a series form. Moreover, by representing the crack as a distribution of dislocation, the existing solutions are used to formulate the logarithmic singular integral equations for a line crack [6,7], and mode-III stress intensity factors are obtained numerically.

The layout of the present paper is as follows. The general formulation for anti-plane elasticity and the method of conformal mapping are introduced in Section 2. The series form solutions for the complex potentials function are given in Section 3. Integral representation for a line crack is established in Section 4. Some numerical examples are solved in Section 5. Finally, Section 6 concludes the article.

2. PROBLEM STATEMENT AND CONFORMAL MAPPING

Consider a cross section of three-phase confocally elliptical composite in an unbounded matrix with arbi-

* Corresponding author (ckchao@mail.ntust.edu.tw)

DOI : 10.1017/jmech.2012.102
Copyright © 2013 The Society of Theoretical and Applied Mechanics, R.O.C.
https://doi.org/10.1017/jmech.2012.102 Published online by Cambridge University Press

trarily oriented crack subjected to a remote uniform shear load as shown on Fig. 1. Let Ω_1 denote the matrix, Ω_2 denote the intermediate layer, and Ω_3 denote the inner inclusion, respectively. The boundaries of intermediate layer are two confocal ellipses Γ_1, Γ_2 with a_1, a_2, and b_1, b_2, being the major and minor semi-axes for each, respectively. Let the medium contain a line crack with length $2c$ and angle β also is located with angle α and distance h from elliptical interface. In addition, let the direction of uniform shear load is 90° from x-axis.

The geometry of the problem is transformed by mapping the confocal ellipse Γ_1, Γ_2 in the z-plane onto the concentric circles L_1, L_2 in the ζ-plane with radii ρ_1, ρ_2 as shown on Fig. 2. The conformal mapping functions is expressed as

$$z = m(\zeta) = \frac{l}{2}\left[R\zeta + \frac{1}{R\zeta}\right] \tag{1}$$

$$R\zeta = \frac{z}{l}\left\{1 + \left[1 - \left(\frac{l}{2}\right)^2\right]^{1/2}\right\} \tag{2}$$

where

$$R = \sqrt{\frac{a_2 + b_2}{a_2 - b_2}} \quad l = \sqrt{a_2^2 - b_2^2} \quad \rho_i = \frac{a_i + b_i}{a_2 + b_2} \quad i = 1,\ 2$$

It also transforms the segment from $-l$ to l in the z-plane onto the circle L_3 of radius $1/R$ in the ζ-plane.

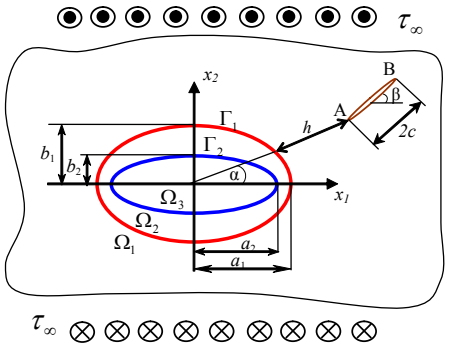


Fig. 1 A three-phase confocally elliptical composite in an unbounded matrix with arbitrarily oriented crack subjected to a remote uniform shear load

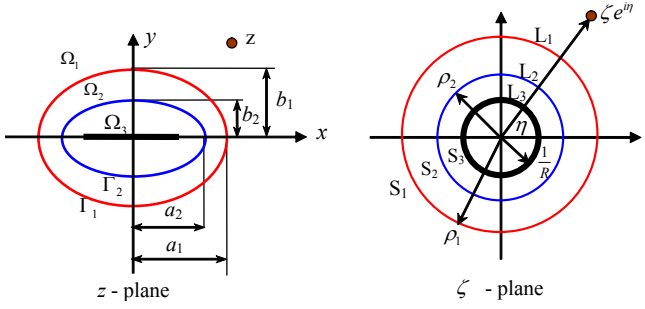


Fig. 2 Conformal mapping from z-plane to ζ-plane

Based on the complex variable theory for a two-dimensional anti-plane elasticity, the resultant force P, displacement ω, and stress component σ_{13} & σ_{23} can be written in terms of a single complex potential $\theta(\zeta)$ as follows

$$P = \int (\sigma_{13} dx_2 - \sigma_{23} dx_1) = -\mu\, \mathrm{Im}\left[\theta(\zeta)\right] \tag{3}$$

$$\omega = \mathrm{Re}\left[\theta(\zeta)\right] \tag{4}$$

$$\sigma_{13} - i\sigma_{23} = \theta'(\zeta) = \Theta(\zeta) \tag{5}$$

$$\sigma_{n3} - i\sigma_{t3} = e^{i\gamma}\Theta(\zeta) \tag{6}$$

where Re and Im denote the real part and imaginary part of the bracketed expression, respectively. The quantities σ_{13}, σ_{23} are the components of shear stresses in x_1 and x_2 direction, respectively, t is the unit tangent of σ, n is the outward unit normal at the interface which in complex form is equal to $e^{i\gamma}$ (where γ is the angle between the normal direction n and the positive axis x_1). (‘) is designated as the derivative with respect to the associated argument and μ stands for the shear modulus. Once the anti-plane problem is solved, the complex potential $\theta(\zeta)$ is determined.

3. COMPLEX POTENTIAL FORMULATION

3.1 Homogeneous Solution

The complex potential for an infinite homogeneous medium subjected to a remote uniform shear load τ_∞ directed at an angle 90° from x-axis is given by the simple expression

$$\theta_0(z) = -i\tau_\infty z \tag{7}$$

With the aid of the mapping function in Eq. (1), the homogeneous solution in the ζ-plane can be rewritten as

$$\theta_0(\zeta) = \frac{-i\tau_\infty l}{2}\left(R\zeta + \frac{1}{R\zeta}\right) \tag{8}$$

In order to solve crack problems, the complex potentials for infinite homogeneous medium corresponding to a screw dislocation with Burgers vector b_z located at $z = z_t$ are introduced as

$$\theta_0(z) = -\frac{ib_z}{2\pi}\log(z - z_t) \tag{9}$$

Similarly, with the aid of mapping function in Eq. (1), the homogeneous solution in the ζ–plane can be written as

$$\theta_0(\zeta) = -\frac{ib_z}{2\pi}\left(\log(\zeta - \zeta_t) + \log\left(1 - \frac{1}{R^2\zeta\zeta_t}\right)\right) \tag{10}$$

Equations (8) and (10) can be rewritten as

$$\theta_0(\zeta) = \theta_{0a}(\zeta) + \theta_{0b}(\zeta) \tag{11}$$

https://doi.org/10.1017/jmech.2012.102 Published online by Cambridge University Press

where the function $\theta_{0a}(\zeta)$ is holomorphic in the region $|\zeta| \le 1$ and the function $\theta_{0b}(\zeta)$ is holomorphic in the region $|\zeta| \ge 1$ respectively.

3.2 Screw Dislocation in Matrix

In this section, we will derive the stress field for a three-phase elliptical composite subjected to a screw dislocation in matrix. The complex potential functions can be assumed as

$$\theta(\zeta)=\begin{cases}\sum_{n=1}^{\infty}\theta_{bn}^{1}(\zeta)+\theta_{0a}(\zeta)+\theta_{0b}(\zeta) & \zeta\in S_1\\ \sum_{n=1}^{\infty}\theta_{an}^{2}(\zeta)+\sum_{n=1}^{\infty}\theta_{bn}^{2}(\zeta) & \zeta\in S_2\\ \sum_{n=1}^{\infty}\theta_{an}^{3}(\zeta)+\sum_{n=1}^{\infty}\theta_{bn}^{3}(\zeta) & \zeta\in S_3\end{cases} \quad (12)$$

where $\theta_{bn}^{1}(\zeta)$ and $\theta_{an}^{2}(\zeta)$ are respectively holomorphic in the regions $|\zeta| \ge \rho_1$ and $|\zeta| \le \rho_1$, $\theta_{bn}^{2}(\zeta)$ and $\theta_{an}^{3}(\zeta)$ are respectively holomorphic in the regions $|\zeta| \ge \rho_2$ and $|\zeta| \le \rho_2$, and $\theta_{bn}^{3}(\zeta)$ is holomorphic in the region $|\zeta| \ge 1/R$, which can be expressed in terms of $\theta_{0a}(\zeta)$ and $\theta_{0b}(\zeta)$. In order to determine the complex potential functions $\theta(\zeta)$ the alternating technique is applied by the following procedure.

Step 1: Analytical Continuation Across the L_1 Interface

First, we introduce two complex functions $\theta_{b1}^{1}(\zeta)$ and $\theta_{a1}^{2}(\zeta)$ respectively holomorphic in $|\zeta| \ge \rho_1$ and $|\zeta| \le \rho_1$ to satisfy the continuity conditions of the displacement and resultant force across the interface L_1 that

$$\theta_{b1}^{1}(t_1)+\theta_{0a}(t_1)+\theta_{0b}(t_1)+\overline{\theta_{b1}^{1}(t_1)}+\overline{\theta_{0a}(t_1)}+\overline{\theta_{0b}(t_1)}=\theta_{a1}^{2}(t_1)+\overline{\theta_{a1}^{2}(t_1)} \quad (13)$$

$$\mu_1\left(\theta_{b1}^{1}(t_1)+\theta_{0a}(t_1)+\theta_{0b}(t_1)-\overline{\theta_{b1}^{1}(t_1)}-\overline{\theta_{0a}(t_1)}-\overline{\theta_{0b}(t_1)}\right)=\mu_2\left(\theta_{a1}^{2}(t_1)-\overline{\theta_{a1}^{2}(t_1)}\right) \quad (14)$$

where $t_1=\rho_1 e^{i\eta}$

By the standard analytical continuation argument and applying Liouville's theorem, we have

$$\begin{cases}\theta_{0a}(\zeta)+\overline{\theta_{0b}}\left(\dfrac{\rho_1^{\,2}}{\zeta}\right)+\overline{\theta_{b1}^{1}}\left(\dfrac{\rho_1^{\,2}}{\zeta}\right)-\theta_{a1}^{2}(\zeta)=0 & |\zeta|\le\rho_1\\ \theta_{b1}^{1}(\zeta)+\overline{\theta_{0a}}\left(\dfrac{\rho_1^{\,2}}{\zeta}\right)+\theta_{0b}(\zeta)-\overline{\theta_{a1}^{2}}\left(\dfrac{\rho_1^{\,2}}{\zeta}\right)=0 & |\zeta|\ge\rho_1\end{cases} \quad (15)$$

$$\begin{cases}\mu_1\theta_{0a}(\zeta)-\mu_1\overline{\theta_{0b}}\left(\dfrac{\rho_1^{\,2}}{\zeta}\right)-\mu_1\overline{\theta_{b1}^{1}}\left(\dfrac{\rho_1^{\,2}}{\zeta}\right)-\mu_2\theta_{a1}^{2}(\zeta)=0\\ \zeta|\le\rho_1\\ \mu_1\overline{\theta_{0a}}\left(\dfrac{\rho_1^{\,2}}{\zeta}\right)-\mu_1\theta_{0b}(\zeta)-\mu_1\theta_{b1}^{1}(\zeta)-\mu_2\overline{\theta_{a1}^{2}}\left(\dfrac{\rho_1^{\,2}}{\zeta}\right)=0\\ \zeta|\ge\rho_1\end{cases} \quad (16)$$

Solve Eqs. (15) and (16) to obtain

$$\theta_{a1}^{2}(\zeta)=U_{21}\theta_{0a}(\zeta) \quad (17)$$

$$\theta_{b1}^{1}(\zeta)=V_{21}\overline{\theta_{0a}}\left(\frac{\rho_1^{\,2}}{\zeta}\right)-\theta_{0b}(\zeta) \quad (18)$$

where $U_{ij}=\dfrac{2\mu_j}{\mu_i+\mu_j}$ $V_{ij}=\dfrac{\mu_j-\mu_i}{\mu_i+\mu_j}$ $i,j=1,2,3$

Since the result of $\theta_{a1}^{2}(\zeta)$ is valid for the region $|\zeta| \le \rho_1$, it cannot satisfy the continuity condition at the interface L_2.

Step 2: Analytical Continuation Across the L_2 Interface

Next, we introduce two functions $\theta_{a1}^{3}(\zeta)$ and $\theta_{b1}^{2}(\zeta)$ respectively holomorphic in $|\zeta| \le \rho_2$ and $|\zeta| \ge \rho_2$ to satisfy the continuity conditions of the displacement and resultant force across the interface L_2 that

$$\theta_{a1}^{2}(t_2)+\theta_{b1}^{2}(t_2)+\overline{\theta_{a1}^{2}(t_2)}+\overline{\theta_{b1}^{2}(t_2)}=\theta_{a1}^{3}(t_2)+\overline{\theta_{a1}^{3}(t_2)} \quad (19)$$

$$\mu_1\left(\theta_{a1}^{2}(t_2)+\theta_{b1}^{2}(t_2)-\overline{\theta_{a1}^{2}(t_2)}-\overline{\theta_{b1}^{2}(t_2)}\right)=\mu_2\left(\theta_{a1}^{3}(t_2)-\overline{\theta_{a1}^{3}(t_2)}\right) \quad (20)$$

where $t_2=\rho_2 e^{i\eta}$

By the analytical continuation method, the solution is found to be

$$\theta_{a1}^{3}(\zeta)=U_{32}\theta_{a1}^{2}(\zeta) \quad (21)$$

$$\theta_{b1}^{2}(\zeta)=V_{32}\overline{\theta_{a1}^{2}}\left(\frac{\rho_2^{2}}{\zeta}\right) \quad (22)$$

But the result of $\theta_{a1}^{3}(\zeta)$ is valid for the region $|\zeta| \le \rho_2$, it cannot satisfy the continuity conditions across L_3. Additional term will be introduced in the third step.

Step 3: Analytical Continuation Across the L_3 Interface

Since the points $t_3=(1/R)e^{i\eta}$ and $\overline{t_3}=(1/R)e^{-i\eta}$ correspond to the same points of the segment from $-l$ to l in the z-plane. The following condition must be satisfied [2]

$$\theta^{3}(t_3)=\theta^{3}(\overline{t_3}) \quad (23)$$

The function $\theta_{b1}^{3}(\zeta)$ holomorphic in $|\zeta| \ge 1/R$ is introduced to satisfy this condition by letting

$$\theta^{3}(\zeta)=\theta_{a1}^{3}(\zeta)+\theta_{b1}^{3}(\zeta) \quad (24)$$

Substitution of Eq. (24) into Eq. (23) yields

$$\theta_{a1}^{3}(t_3)+\theta_{b1}^{3}(t_3)=\theta_{a1}^{3}(\overline{t_3})+\theta_{b1}^{3}(\overline{t_3}) \quad (25)$$

By the analytical continuation method, the solution is found to be

https://doi.org/10.1017/jmech.2012.102 Published online by Cambridge University Press

$$\theta_{b1}^{3}(\zeta)=\theta_{a1}^{3}\left(\frac{1}{R^{2}\zeta}\right) \tag{26}$$

Step 4: Analytical Continuation Across the L_1 Interface

Two additional functions $\theta_{b2}^{1}(\zeta)$ and $\theta_{a2}^{2}(\zeta)$ respectively holomorphic in $|\zeta| \geq \rho_1$ and $|\zeta| \leq \rho_1$ are introduced to satisfy the continuity conditions across the interface L_1 that

$$\theta_{b2}^{1}(t_1)+\overline{\theta_{b2}^{1}(t_1)}=\theta_{b1}^{2}(t_1)+\theta_{a2}^{2}(t_1)+\overline{\theta_{b1}^{2}(t_1)}+\overline{\theta_{a2}^{2}(t_1)} \tag{27}$$

$$\mu_1\left(\theta_{b2}^{1}(t_1)-\overline{\theta_{b2}^{1}(t_1)}\right)=\mu_2\left(\theta_{b1}^{2}(t_1)+\theta_{a2}^{2}(t_1)-\overline{\theta_{b1}^{2}(t_1)}-\overline{\theta_{a2}^{2}(t_1)}\right) \tag{28}$$

where $t_1=\rho_1 e^{i\eta}$

By the same method, we have

$$\theta_{a2}^{2}(\zeta)=V_{12}\overline{\theta_{b1}^{2}}\left(\frac{\rho_1^{\,2}}{\zeta}\right) \tag{29}$$

$$\theta_{b2}^{1}(\zeta)=U_{12}\theta_{b1}^{2}(\zeta) \tag{30}$$

Step 5: Repetitions of Steps 2, 3 and 4

The method of analytical continuation is repeatedly performed across each interface to achieve the unknown functions $\theta_{a2}^{3}(\zeta)$, $\theta_{b2}^{3}(\zeta)$, $\theta_{bn}^{1}(\zeta)$, $\theta_{an}^{2}(\zeta)$, $\theta_{bn}^{2}(\zeta)$, $\theta_{an}^{3}(\zeta)$, and $\theta_{bn}^{3}(\zeta)$ (n = 3, 4, 5, …). Consequently, one can express all the functions in terms of $\theta_{0a}(\zeta)$ and $\theta_{0b}(\zeta)$ as follows

$$\begin{cases}\theta_{b1}^{1}(\zeta)=V_{21}\overline{\theta_{0a}}\left(\dfrac{\rho_1^{\,2}}{\zeta}\right)-\theta_{0b}(\zeta)\\ \theta_{a1}^{2}(\zeta)=U_{21}\theta_{0a}(\zeta)\\ \theta_{b1}^{2}(\zeta)=V_{32}U_{21}\overline{\theta_{0a}}\left(\dfrac{\rho_2^{\,2}}{\zeta}\right)\\ \theta_{a1}^{3}(\zeta)=U_{32}U_{21}\theta_{0a}(\zeta)\\ \theta_{b1}^{3}(\zeta)=U_{32}U_{21}\theta_{0a}\left(\dfrac{1}{R^{2}\zeta}\right)\end{cases} \tag{31a}$$

and

$$\begin{cases}\theta_{bn}^{1}(\zeta)=U_{12}\theta_{b(n-1)}^{2}(\zeta)\\ \theta_{bn}^{2}(\zeta)=V_{32}V_{12}\theta_{b(n-1)}^{2}\left(\dfrac{\rho_1^2}{\rho_2^2}\zeta\right)+U_{23}\theta_{a(n-1)}^{3}\left(\dfrac{1}{R^{2}\zeta}\right)\\ \theta_{bn}^{3}(\zeta)=V_{23}\overline{\theta_{a(n-1)}^{3}}\left(\dfrac{1}{R^{4}\rho_2^{2}\zeta}\right)+U_{32}V_{12}\overline{\theta_{b(n-1)}^{2}}(R^{2}\rho_1^{2}\zeta)\\ \theta_{an}^{2}(\zeta)=V_{12}\overline{\theta_{b(n-1)}^{2}}\left(\dfrac{\rho_1^2}{\zeta}\right)\\ \theta_{an}^{3}(\zeta)=V_{23}\overline{\theta_{a(n-1)}^{3}}\left(\dfrac{1}{R^{2}\rho_2^{2}}\zeta\right)+U_{32}V_{12}\overline{\theta_{b(n-1)}^{2}}\left(\dfrac{\rho_1^2}{\zeta}\right)\end{cases} \tag{31b}$$

for $n \geq 2$

The complete solution for three-phase elliptical composite subjected to screw dislocation in matrix can be obtained by substituting Eqs. (9), (10) and (31) into Eq. (12)

3.3 Screw Dislocation in Intermediate Layer

When a screw dislocation is located in S_2, the problem becomes more difficult to solve. To satisfy the single-valued conditions of displacements and resultant force, the complex potential function should have the form

$$\theta(\zeta)=\begin{cases}\dfrac{-i\mu_1 b_z}{2\pi}\log\dfrac{\zeta}{\rho_1}+\sum\limits_{n=1}^{\infty}\theta_{bn}^{1}(\zeta) & \zeta\in S_1\\ \theta_{0a}(\zeta)+\theta_{0b}(\zeta)+\sum\limits_{n=1}^{\infty}\theta_{an}^{2}(\zeta)+\sum\limits_{n=1}^{\infty}\theta_{bn}^{2}(\zeta) & \zeta\in S_2\\ \sum\limits_{n=1}^{\infty}\theta_{an}^{3}(\zeta)+\sum\limits_{n=1}^{\infty}\theta_{bn}^{3}(\zeta) & \zeta\in S_3\end{cases} \tag{32}$$

By the same arguments as in case of screw dislocation in matrix, the alternating technique is applied to solve the current problem.

Step 1: Analytical Continuation Across the L_1 Interface

First, we introduce two complex functions $\theta_{b1}^{1}(\zeta)$ and $\theta_{a1}^{2}(\zeta)$ respectively holomorphic in $|\zeta| \geq \rho_1$ and $|\zeta| \leq \rho_1$ to satisfy the continuity conditions of the displacement and resultant force across the interface L_1 that

$$\theta_{b1}^{1}(t_1)+\overline{\theta_{b1}^{1}(t_1)}=\theta_{00}(\zeta)+\overline{\theta_{00}(\zeta)}+\theta_{a1}^{2}(t_1)+\overline{\theta_{a1}^{2}(t_1)} \tag{33}$$

$$\mu_1\left(\theta_{b1}^{1}(t_1)-\overline{\theta_{b1}^{1}(t_1)}\right)=\mu_2\left(\theta_{00}(\zeta)-\overline{\theta_{00}(\zeta)}+\theta_{a1}^{2}(t_1)-\overline{\theta_{a1}^{2}(t_1)}\right) \tag{34}$$

where $t_1=\rho_1 e^{i\eta}$ and

$$\theta_{00}(\zeta)=-\frac{i\mu_2 b_z}{2\pi}\log\left(\left(1-\frac{\zeta_t}{\zeta}\right)\left(1-\frac{1}{R^{2}\zeta\zeta_t}\right)\right)$$

By the analytical continuation method, we have

$$\theta_{b1}^{1}(\zeta)=U_{12}\theta_{00}(\zeta) \tag{35}$$

$$\theta_{a1}^{2}(\zeta)=V_{12}\overline{\theta_{00}}\left(\frac{\rho_1^{\,2}}{\zeta}\right) \tag{36}$$

Since the result of $\theta_{a1}^{2}(\zeta)$ is valid for the region $|\zeta| \leq \rho_1$, it cannot satisfy the continuity condition at the interface L_2.

Step 2: Analytical Continuation Across the L_2 Interface

Next, we introduce two functions $\theta_{a1}^{3}(\zeta)$ and $\theta_{b1}^{2}(\zeta)$ respectively holomorphic in $|\zeta| \leq \rho_2$ and $|\zeta| \geq \rho_2$ to satisfy the continuity conditions of the displacement and resultant force across the interface L_2 that

https://doi.org/10.1017/jmech.2012.102 Published online by Cambridge University Press

$$\theta_{a1}^2(t_2)+\theta_{b1}^2(t_2)+\theta_0(t_2)+\overline{\theta_{a1}^2(t_2)}+\overline{\theta_{b1}^2(t_2)}+\overline{\theta_0(t_2)} = \theta_{a1}^3(t_2)+\overline{\theta_{a1}^3(t_2)} \tag{37}$$

$$\mu_2\left(\theta_{a1}^2(t_2)+\theta_{b1}^2(t_2)+\theta_0(t_2)-\overline{\theta_{a1}^2(t_2)}-\overline{\theta_{b1}^2(t_2)}-\overline{\theta_0(t_2)}\right) = \mu_3\left(\theta_{a1}^3(t_2)-\overline{\theta_{a1}^3(t_2)}\right) \tag{38}$$

where $t_2 = \rho_2 e^{i\eta}$

By the analytical continuation method, the solution is found to be

$$\theta_{b1}^2(\zeta) = V_{32}\left(\overline{\theta_{a1}^2}\left(\frac{\rho_2^2}{\zeta}\right)+\overline{\theta_{0a}}\left(\frac{\rho_2^2}{\zeta}\right)\right)-\theta_{0b}(\zeta) \tag{39}$$

$$\theta_{a1}^3(\zeta) = U_{32}\left(\theta_{a1}^2(\zeta)+\theta_{0a}(\zeta)\right) \tag{40}$$

Step 3: Repetitions of Previous Steps

The method of analytical continuation is repeatedly performed across each interface to achieve the unknown functions $\theta_{b1}^3(\zeta)$, $\theta_{bn}^1(\zeta)$, $\theta_{an}^2(\zeta)$, $\theta_{bn}^2(\zeta)$, $\theta_{an}^3(\zeta)$, and $\theta_{bn}^3(\zeta)$ (n = 2, 3, 4, …). Consequently, one can find the complete solution of $\theta(\zeta)$ as follows

$$\begin{cases}\theta_{b1}^1(\zeta) = U_{12}\theta_{00}(\zeta)\\ \theta_{a1}^2(\zeta) = V_{12}\overline{\theta_{00}}\left(\dfrac{\rho_1^2}{\zeta}\right)\\ \theta_{b1}^2(\zeta) = V_{32}\left(\overline{\theta_{a1}^2}\left(\dfrac{\rho_2^2}{\zeta}\right)+\overline{\theta_{0a}}\left(\dfrac{\rho_2^2}{\zeta}\right)\right)-\theta_{0b}(\zeta)\\ \theta_{a1}^3(\zeta) = U_{32}\left(\theta_{a1}^2(\zeta)+\theta_{0a}(\zeta)\right)\\ \theta_{b1}^3(\zeta) = U_{32}\left(\theta_{a1}^2\left(\dfrac{1}{R^2\zeta}\right)+\theta_{0a}\left(\dfrac{1}{R^2\zeta}\right)\right)\end{cases} \tag{41a}$$

and

$$\begin{cases}\theta_{bn}^1(\zeta) = U_{12}\theta_{b(n-1)}^2(\zeta)\\ \theta_{an}^2(\zeta) = V_{12}\overline{\theta_{b(n-1)}^2}\left(\dfrac{\rho_1^2}{\zeta}\right)\\ \theta_{bn}^2(\zeta) = V_{32}\overline{\theta_{an}^2}\left(\dfrac{\rho_2^2}{\zeta}\right)+U_{23}\theta_{a(n-1)}^3\left(\dfrac{1}{R^2\zeta}\right)\\ \theta_{an}^3(\zeta) = U_{32}\theta_{an}^2(\zeta)+V_{23}\overline{\theta_{a(n-1)}^3}\left(\dfrac{1}{R^2\rho_2^2}\zeta\right)\\ \theta_{bn}^3(\zeta) = U_{32}V_{12}\overline{\theta_{b(n-1)}^2}\left(R^2\rho_1^2\zeta\right)+V_{23}\overline{\theta_{a(n-1)}^3}\left(\dfrac{1}{R^4\rho_2^2\zeta}\right)\end{cases} \tag{41b}$$

for $n \geq 2$

The complete solution for three-phase elliptical composite subjected to screw dislocation in intermediate layer can be obtained by substituting Eqs. (9), (10) and (41) into Eq. (32)

3.4 Screw Dislocation in Inner Inclusion

To satisfy the single-valued conditions of displacements and resultant force, the complex potential function should have the form

$$\theta(\zeta) = \begin{cases}\dfrac{-i\mu_1 b_z}{2\pi}\log\dfrac{\zeta}{\rho_1}+\sum\limits_{n=1}^{\infty}\theta_{bn}^1(\zeta) & \zeta\in S_1\\ \dfrac{-i\mu_2 b_z}{2\pi}\log\dfrac{\zeta}{\rho_2}+\sum\limits_{n=1}^{\infty}\theta_{an}^2(\zeta)+\sum\limits_{n=1}^{\infty}\theta_{bn}^2(\zeta) & \zeta\in S_2\\ \theta_{0a}(\zeta)+\theta_{0b}(\zeta)+\sum\limits_{n=1}^{\infty}\theta_{an}^3(\zeta)+\sum\limits_{n=1}^{\infty}\theta_{bn}^3(\zeta) & \zeta\in S_3\end{cases} \tag{42}$$

By a similar way to the previous approach, we can find

$$\begin{cases}\theta_{b1}^3(\zeta) = \theta_{0a}\left(\dfrac{1}{R^2\zeta}\right)-\theta_{0a}(\zeta)\\ \theta_{b1}^2(\zeta) = U_{23}\left(\theta_{b1}^3(\zeta)+\theta_{00}(\zeta)\right)\\ \theta_{b1}^1(\zeta) = U_{12}\theta_{b1}^2(\zeta)\\ \theta_{a1}^2(\zeta) = V_{12}\overline{\theta_{b1}^2}\left(\dfrac{\rho_1^2}{\zeta}\right)\\ \theta_{a1}^3(\zeta) = V_{23}\left(\overline{\theta_{b1}^3}\left(\dfrac{\rho_2^2}{\zeta}\right)+\overline{\theta_{00}}\left(\dfrac{\rho_2^2}{\zeta}\right)\right)\end{cases} \tag{43a}$$

and

$$\begin{cases}\theta_{bn}^3(\zeta) = \theta_{a(n-1)}^3\left(\dfrac{1}{R^2\zeta}\right)\\ \theta_{bn}^2(\zeta) = U_{23}\theta_{bn}^3(\zeta)+V_{32}V_{12}\theta_{b(n-1)}^2\left(\dfrac{\rho_1^2}{\rho_2^2}\zeta\right)\\ \theta_{bn}^1(\zeta) = U_{12}\theta_{bn}^2(\zeta)\\ \theta_{an}^2(\zeta) = V_{12}\overline{\theta_{bn}^2}\left(\dfrac{\rho_1^2}{\zeta}\right)\\ \theta_{an}^3(\zeta) = V_{23}\overline{\theta_{bn}^3}\left(\dfrac{\rho_2^2}{\zeta}\right)+U_{32}V_{12}\overline{\theta_{b(n-1)}^2}\left(\dfrac{\rho_1^2}{\zeta}\right)\end{cases} \tag{43b}$$

for $n \geq 2$

The complete solution for three-phase elliptical composite subjected to screw dislocation in matrix can be obtained by substituting Eqs. (9), (10) and (43) into Eq. (42).

4. INTEGRAL EQUATIONS

The singular integral equations for this problem can easily be written down by using the dislocation solutions as the Green's function together with the principle of superposition.

First, to model the crack embedded in the infinite matrix it is necessary to place a dislocation distribution $b_z(s)$ along the prospective site of the crack. In this case, we simply substitute b_z by $b_z(s)$ and make integra-

https://doi.org/10.1017/jmech.2012.102 Published online by Cambridge University Press

tion along the crack. The corresponding homogeneous solution associated with a single crack can be expressed as

$$\theta_{0a}(\zeta) = -\frac{i\mu_1}{2\pi}\int_L b_z(s)\log(\zeta-\zeta_t)\,ds \tag{44}$$

$$\theta_{0b}(\zeta) = -\frac{i\mu_1}{2\pi}\int_L b_z(s)\log\left(1-\frac{1}{R^2\zeta\zeta_t}\right)ds \tag{45}$$

where $b_z(s)$ indicate the density function and ζ_t is a point on the crack.

The principle of superposition can be applied due to the traction-free condition along the crack surface. It means, the total resultant force across the crack surface must be balance by the given resultant force across the crack segment in the unflawed media, *i.e.*

$$p(\zeta) = -p^{\infty}(\zeta) \tag{46}$$

where the resultant force applied on the crack surface will be obtained by substituting Eqs. (12_1), (44) and (45) into Eq. (3) as follows

$$p(\zeta) = -\mu_1\left[-\frac{i\mu_1}{2\pi}\left(\int_L b_z(s)\log(\zeta-\zeta_t)\,ds + \int_L b_z(s)\log\left(1-\frac{1}{R^2\zeta\zeta_t}\right)ds\right)+\sum_{n=1}^{\infty}\theta_{bn}^1(\zeta)\right] \tag{47}$$

On the other hand, the resultant force corresponding to the unflawed media can be obtained by substituting Eqs. (8) and (12_1) into Eq. (3) as follows

$$p^{\infty}(\zeta) = -\mu_1\left[\frac{-i\tau_{\infty}l}{2}\left(R\zeta+\frac{1}{R\zeta}\right)+\sum_{n=1}^{\infty}\theta_{bn}^1(\zeta)\right] \tag{48}$$

In addition, the single-valued condition of the dislocation density must be satisfied, *i.e.*

$$\int_L b_0(s)\,ds = 0 \tag{49}$$

In order to obtain the unknown function $b_z(s)$, the singular integral equation from Eqs. (46), (47), and (48) together with the subsidiary condition Eq. (49) may be solved numerically. After obtaining the unknown function $b_z(s)$, the mode-III stress intensity factors can be obtained accordingly as

$$K_{III}(tip-A) = -\sqrt{\pi}\lim_{s_1\to 0} b_z(s_1)\,s_1^{1/2} = -\sqrt{\pi d_1}\,b_{z,1} \tag{50}$$

$$K_{III}(tip-B) = \sqrt{\pi}\lim_{s_{N+1}\to 2d} b_z(s_{N+1})\,s_{N+1}^{1/2} = \sqrt{\pi d_N}\,b_{z,N+1} \tag{51}$$

For a crack located in the intermediate layer, the corresponding homogeneous solution associated with a single crack can be expressed as

$$\theta_{0a}(\zeta) = -\frac{i\mu_2}{2\pi}\int_L b_z(s)\log(\zeta-\zeta_t)\,ds \tag{52}$$

$$\theta_{0b}(\zeta) = -\frac{i\mu_2}{2\pi}\int_L b_z(s)\log\left(1-\frac{1}{R^2\zeta\zeta_t}\right)ds \tag{53}$$

$$\theta_{00}(\zeta) = -\frac{i\mu_2}{2\pi}\int_L b_z(s)\log\left(\left(1-\frac{\zeta_t}{\zeta}\right)\left(1-\frac{1}{R^2\zeta\zeta_t}\right)\right)ds \tag{54}$$

The resultant force applied on the crack surface will be obtained by substituting Eqs. (32_2), (52), (53) and (54) into Eq. (3) as follows

$$p(\zeta) = -\mu_2\left[-\frac{i\mu_2}{2\pi}\left(\int_L b_z(s)\log(\zeta-\zeta_t)\,ds+\int_L b_z(s)\log\left(1-\frac{1}{R^2\zeta\zeta_t}\right)ds\right)+\sum_{n=1}^{\infty}\theta_{an}^2(\zeta)+\sum_{n=1}^{\infty}\theta_{bn}^2(\zeta)\right] \tag{55}$$

On the other hand, the resultant force corresponding to the unflawed media can be obtained by substituting Eqs. (8) and (12_2) into Eq. (3) as follows

$$p^{\infty}(\zeta) = -\mu_2\left[\sum_{n=1}^{\infty}\theta_{an}^2(\zeta)+\sum_{n=1}^{\infty}\theta_{bn}^2(\zeta)\right] \tag{56}$$

The unknown function $b_z(s)$ for a crack located in the intermediate layer can be obtained numerically by using the Eqs. (46), (55), and (56) together with Eq. (47). Accordingly, the mode-III stress intensity factors can also be obtained from Eqs. (50) and (51).

For a crack located in the inner inclusion, the corresponding homogeneous solution associated with a single crack can be expressed as

$$\theta_{0a}(\zeta) = -\frac{i\mu_3}{2\pi}\int_L b_z(s)\log(\zeta-\zeta_t)\,ds \tag{57}$$

$$\theta_{0b}(\zeta) = -\frac{i\mu_3}{2\pi}\int_L b_z(s)\log\left(1-\frac{1}{R^2\zeta\zeta_t}\right)ds \tag{58}$$

$$\theta_{00}(\zeta) = -\frac{i\mu_3}{2\pi}\int_L b_z(s)\log\left(\left(1-\frac{\zeta_t}{\zeta}\right)\left(1-\frac{1}{R^2\zeta\zeta_t}\right)\right)ds \tag{59}$$

The resultant force applied on the crack surface will be obtained by substituting Eqs. (42^3), (57), (58) and (59) into Eq. (3) as follows

$$p(\zeta) = -\mu_3\left[-\frac{i\mu_3}{2\pi}\left(\int_L b_z(s)\log(\zeta-\zeta_t)\,ds+\int_L b_z(s)\log\left(1-\frac{1}{R^2\zeta\zeta_t}\right)ds\right)+\sum_{n=1}^{\infty}\theta_{an}^3(\zeta)+\sum_{n=1}^{\infty}\theta_{bn}^3(\zeta)\right] \tag{60}$$

On the other hand, the resultant force corresponding to the unflawed media can be obtained by substituting Eqs. (8) and (12^3) into Eq. (3) as follows

https://doi.org/10.1017/jmech.2012.102 Published online by Cambridge University Press

$$p^{\infty}(\zeta) = -\mu_3 \left[\sum_{n=1}^{\infty} \theta_{an}^3(\zeta) + \sum_{n=1}^{\infty} \theta_{bn}^3(\zeta) \right] \qquad (61)$$

The unknown function $b_z(s)$ for a crack located in the inner inclusion can be obtained numerically by using the Eqs. (46), (60), and (61) together with Eq. (47). Accordingly, the mode-III stress intensity factors can also be obtained from Eqs. (50) and (51).

5. RESULTS AND DISCUSSION

The major purpose of this present paper is to analyze the interaction between a crack and an elliptically cylindrical layered media under a remote uniform shear load. This can be achieved by the determination of the stress intensity factors that may properly characterize the interaction behavior between a crack and an elliptically cylindrical layered media. In the following results, only three cases shown in Fig. 3, respectively, have been considered.

5.1 A Crack Located in Matrix

It is well known that for two-phase composite, a softer inclusion will give enhancement effect on stress intensity factors when a crack approaching the interface. On the other hand, a stiffer inclusion will give retardation effect because it may tend to act as a barrier in load transfer. In this section, we will investigate the effect of material property combination of intermediate layer and inner inclusion on stress intensity factors in three-phase composite with a crack placed in the matrix.

The variation of dimensionless mode-III stress intensity factors (K_{III}^*(tip-A) $= K_{III}$(tip-A)/ $\tau_\infty \sqrt{\pi c}$) versus dimensionless location of a crack (h/a_2) for different material property combinations are shown in Figs. 4 ~ 7, respectively. In this case, the geometric configurations are considered as $b_2 / a_2 = 0.8$, $a_1 / a_2 = 1.1$ for a confocal ellipse and $c/a_2 = 0.1$, $\alpha = \beta = 0°$ for a crack.

Figures 4 ~ 5 show that the existence of a hard (soft) material property in both intermediate layer and inner inclusion will give the retardation (enhancement) effect on K_{III}^*(tip-A). This applies to the behavior of two-phase composite.

Figure 6 shows that a three-phase composite system with material property of intermediate layer a half softer than matrix ($\mu_2 / \mu_1 = 0.5$) does not always give enhancement effect on K_{III}^*(tip-A) like the behavior in two-phase composite. It is interesting to see that a stiffer inclusion ($\mu_3 / \mu_1 = 4$) will give retardation effect even when the intermediate layer is softer than the matrix. Similar observations can also be applied to a three-phase composite system with ($\mu_3 / \mu_1 = 0.5$) as shown in Fig. 7. From Fig. 7, we see that the presence of a stiffer intermediate layer ($\mu_2 / \mu_1 \geq 3$) will give retardation effect on K_{III}^*(tip-A) even when the inclusion is softer than the matrix. Those behaviors can be much clearly interpreted by using the diagram as seen in the Fig. 8. Region I (or Region III) represents the

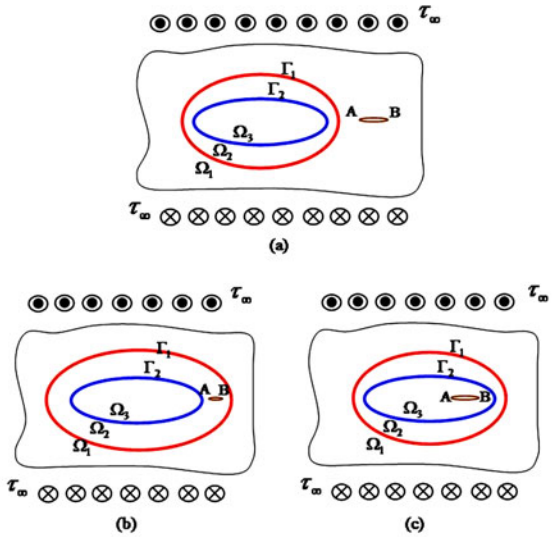


Fig. 3 A three-phase confocally elliptical composite with a crack in x-axis and located in (a) an infinite matrix (b) an intermediate layer (c) an inner inclusion

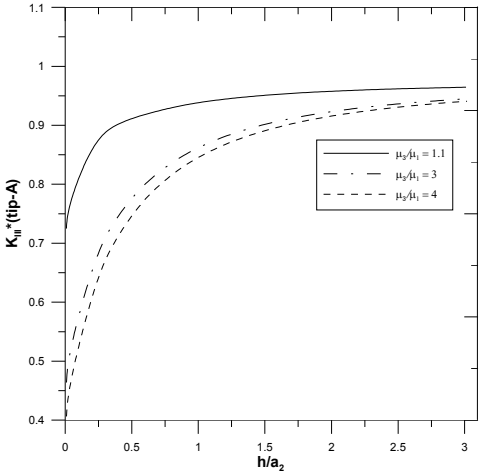


Fig. 4 Mode-III stress intensity factors at tip A versus location of a crack for different material property combinations ($\mu_2 / \mu_1 = 2$)

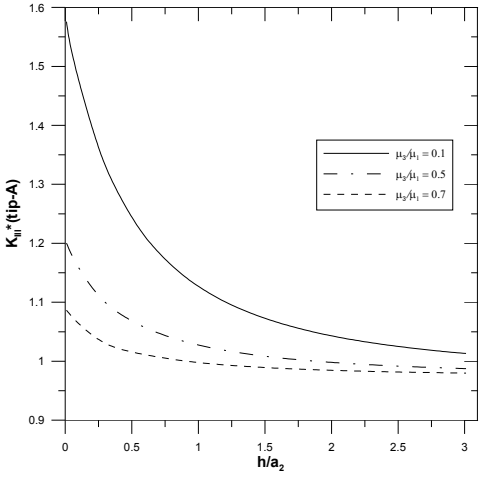


Fig. 5 Mode-III stress intensity factors at tip A versus location of a crack for different material property combinations ($\mu_3 / \mu_1 = 0.9$)

https://doi.org/10.1017/jmech.2012.102 Published online by Cambridge University Press

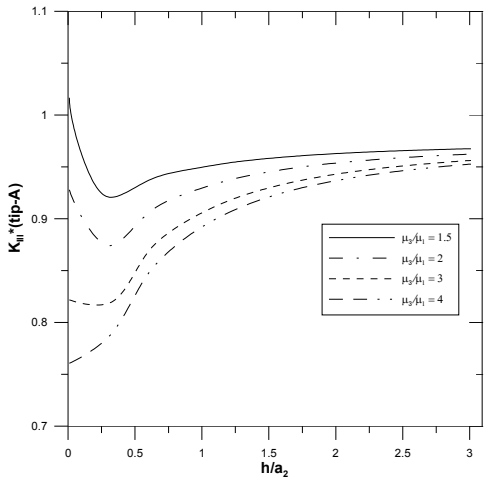


Fig. 6 Mode-III stress intensity factors at tip A versus location of a crack for different material property combinations ($\mu_2 / \mu_1 = 0.5$)

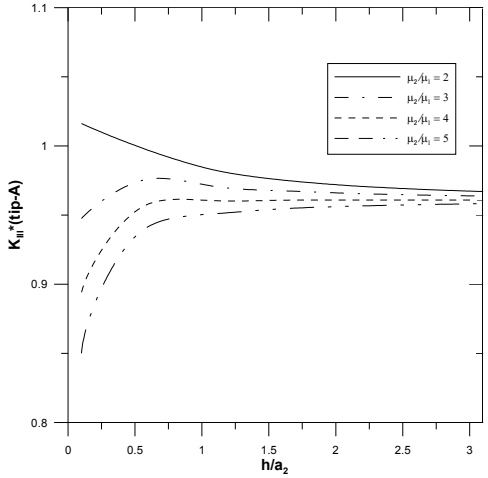


Fig. 7 Mode-III stress intensity factors at tip A versus location of a crack for different material property combinations ($\mu_3 / \mu_1 = 0.5$)

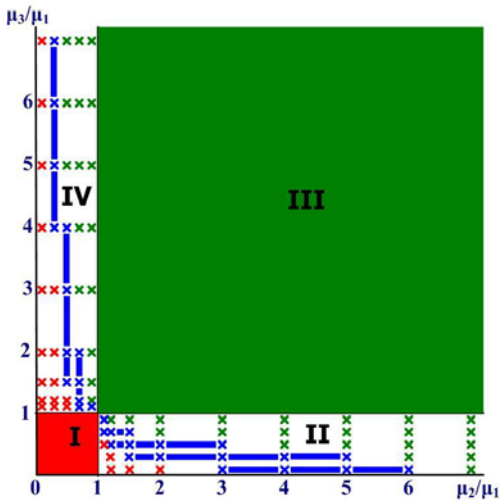


Fig. 8 Diagram of material property effect for mode III- stress intensity factors at tip A in three-phase elliptical composite interacting with a crack located in matrix

behavior of K_{III}^*(tip-A) when both intermediate layer and inner inclusion are softer (or stiffer) than the matrix. One can see that the material property combinations in Region I always give enhancement effect while the material property combinations in region III always give retardation effect on K_{III}^*(tip-A).

Region II (or IV) represents the behavior of K_{III}^*(tip-A) when an intermediate layer is stiffer (or softer) than the matrix while the inner inclusion is softer (or stiffer) than the matrix. In these two regions, we can find the mixing behavior represented in blue area that separates the green area (retardation effect) from the red area (enhancement effect). This mixing behavior actually is the transition from enhancement effect into retardation effect due to the presence of stiffer intermediate layer or stiffer inner inclusion. It is noted that a very soft intermediate layer (inner inclusion) should be combined with a very stiff inner inclusion (intermediate layer) in order to achieve the mixing behavior.

5.2 A Crack Located in Intermediate Layer

The variation of dimensionless mode-III stress intensity factors versus dimensionless location of a crack (h / a_2) for different material property combinations are shown in Figs. 9 ~ 10. In this case, the geometric conditions are represented by $b_2 / a_2 = 0.8$, $a_1 / a_2 = 1.3$ for a confocal ellipse and $c/a_2 = 0.1$, $\alpha = \beta = 0°$ for a crack. Figure 9 shows that the existence of a stiffer (or softer) intermediate layer compared to the inclusion may give the enhancement (or retardation) effect on K_{III}^*(tip-A) when a crack is approaching the inner inclusion. Figure 10 shows that the existence of a softer matrix compared to the intermediate layer may always give the enhancement effect on K_{III}^*(tip-B).

5.3 A Crack Located in Inner Inclusion

The variation of dimensionless mode-III stress intensity factors K_{III}^*(tip-B)) versus dimensionless location of a crack (h / a_2) for different material property combinations are shown in Fig. 11. In this case, the geometric configurations are represented by $b_2 / a_2 = 0.8$, $a_1 / a_2 = 1.1$ for a confocal ellipse and $c/a_2 = 0.1$, $\alpha = \beta = 0°$ for a crack. Figure 11 shows that the existence of a stiffer (or softer) inclusion compared to the intermediate layer may give the enhancement (or retardation) effect on K_{III}^*(tip-B) when a crack is approaching to the intermediate layer.

6. CONCLUSIONS

An analytical exact solution of interaction between a line crack with an elliptically cylindrical layered media under a remote uniform shear load is presented in this paper. By applying the existing complex potential solutions for a dislocation function, the logarithmic singular integral equations for a line crack in an infinite matrix, intermediate layer, and inner inclusion are formulated. Numerical calculations are performed to investigate the effect of material properties combinations on mode-III stress intensity factors.

https://doi.org/10.1017/jmech.2012.102 Published online by Cambridge University Press

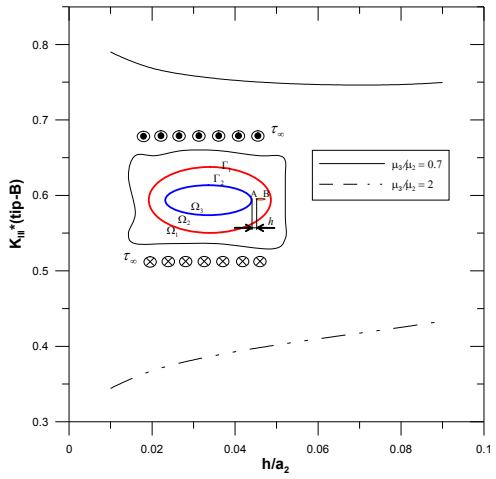


Fig. 9 Mode-III stress intensity factors at tip A versus location of a crack for different material property combinations (μ1/μ2 = 0.5)

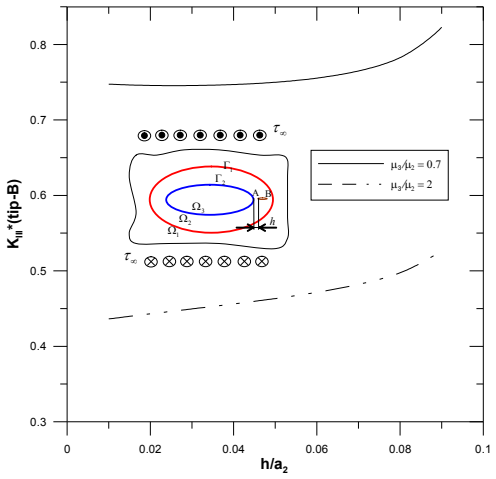


Fig. 10 Mode-III stress intensity factors at tip B versus location of a crack for different material property combinations ($\mu_1 / \mu_2 = 0.5$)

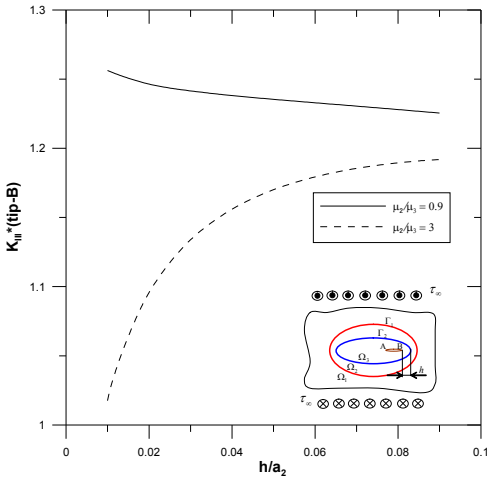


Fig. 11 Mode-III stress intensity factors at tip B versus location of a crack for different material property combinations ($\mu_1 / \mu_3 = 2$)

REFERENCES

1. Chao, C. K., Wikarta, A. and Korsunsky, A. M., "Anti-Plane Interaction of a Crack and Reinforced Elliptic Hole in an Infinite Matrix," *Theoretical and Applied Fracture Mechanics*, **53**, pp. 205–210 (2010).
2. Stagni, L. and Lizzio, R., "Shape Effects in the Interaction Between an Edge Dislocation and an Elliptical Inhomogeneity," *Applied Physics A: Materials Science & Processing*, **30**, pp. 217–221 (1983).
3. Ru, C. Q., "Effect of Interphase Layers on Thermal Stresses Within an Elliptical Inclusion," *Journal of Applied Physics*, **84**, pp. 4872–4879 (1998).
4. Ru, C. Q., Schiavone, P. and Mioduchowski, A., "Uniformity of Stresses Within a Three-Phase Elliptic Inclusion in Anti-Plane Shear," *Journal of Elasticity*, **52**, pp. 121–128 (1999).
5. Shen, M. H., Chen, S. N. and Chen, F. M., "Anti-plane Study on Confocally Elliptical Inhomogeneity Problem Using an Alternating Technique," *Archives of Applied Mechanics*, **75**, pp. 302–314 (2006).
6. Chao, C. K. and Shen, M. H., "Solutions of Thermoelastic Crack Problems in Bonded Dissimilar Media or Half-Plane Medium," *International Journal of Solids and Structures*, **32**, pp. 3537–3554 (1995).
7. Chao, C. K. and Lee, J. Y., "Interaction Between a Crack and a Circular Elastic Inclusion Under Remote Uniform Heat Flow," *International Journal of Solids and Structures*, **33**, pp. 3865–3880 (1996).

(Manuscript received December 8, 2011, accepted for publication February 8, 2012.)

https://doi.org/10.1017/jmech.2012.102 Published online by Cambridge University Press